Earth and Planetary Science Letters 345–348 (2012) 81–89

Contents lists available at SciVerse ScienceDirect

Earth and Planetary Science Letters

journal homepage: www.elsevier.com/locate/epsl

Letters

Reaction-driven cracking during retrograde metamorphism: Olivine hydration and carbonation

Peter B. Kelemen [a,*], Greg Hirth [b]

[a] Lamont Doherty Earth Observatory, Columbia University, Palisades, NY 10964, USA
[b] Department of Geological Sciences, Brown University, Providence, RI 02912, USA

ARTICLE INFO

Article history:
Received 10 February 2012
Received in revised form
7 June 2012
Accepted 10 June 2012
Editor: Y. Ricard

Keywords:
peridotite alteration
serpentinization
mineral carbonation
reaction-driven cracking
pressure of crystallization
CO_2 capture and storage

ABSTRACT

Retrograde metamorphism (mineral hydration, carbonation and oxidation) is important in controlling the composition and rheology of the Earth's crust and upper mantle, particularly along tectonic plate margins, and in proposed mechanisms for geothermal power generation and engineered, geological carbon storage. Retrograde processes can lead to an increase in solid mass and volume, or can be balanced by host phase dissolution at constant solid volume. In turn, solid volume changes could reduce permeability and reactive surface area, and/or lead to host rock deformation, via fracture and frictional sliding or viscous flow. Which of these outcomes emerges in specific cases is determined in part by the "crystallization pressure", which creates local gradients in pressure around growing crystals, and thus a differential stress. We develop thermodynamic and mineral physics estimates of the crystallization pressure and differential stress resulting from volume changes during olivine hydration (serpentinization) and carbonation. Because olivine is so far from equilibrium with fluids near the surface, the stress due to serpentinization and/or carbonation may exceed 300 MPa at temperatures up to 200 °C or more, greater than required to fracture rocks and cause frictional failure in the upper 10 km of the Earth. Provided that fluid access is initiated, for example along pre-existing fractures, the volume change due to hydration and carbonation can cause fracture formation and dilation, maintaining or increasing permeability and reactive surface energy in a positive feedback mechanism.

1. Retrograde metamorphism of mantle olivine

Retrograde metamorphism – hydration, carbonation and oxidation of igneous and metamorphic rocks – is an essential process in Earth dynamics. In situ retrograde reactions, where the volatile-rich product phase occupies the same location as the volatile-poor reactant phase, are commonly referred to as replacement reactions. Retrograde replacement of olivine ($(Mg,Fe)_2SiO_4$) by serpentine ($(Mg,Fe)_3Si_2O_5(OH)_4$) and/or magnesite ($(Mg,Fe)CO_3$) is the focus of this paper.

Typical residual mantle peridotite in ophiolites and mid-ocean ridge peridotites is composed of 70–85% olivine, plus 5–15% dunite in bands containing more than 95% olivine. Peridotite alteration occurs at appreciable rates near the surface. For example, in their classic paper Barnes and O'Neil (1969) estimated that dissolved Ca in a single, small alkaline spring was extracted during serpentinization of 10^3–10^4 t of peridotite per year. In the upper crust, at ~200 MPa, mantle peridotite is unstable in the presence of water below ~700 °C (Evans, 1977), and unstable in the presence of CO_2-rich fluids below ~500 °C (Johannes, 1969). The Fe component in olivine is unstable at the high oxygen fugacity that prevails near the Earth's surface (Frost, 1985). At near-surface temperatures, e.g., 50 °C, the energy density (free energy per unit mass) for olivine hydration, carbonation and oxidation is of the order of 500 kJ/kg, about 1% of the energy density for liquid hydrocarbon fuels.

Tectonic processes – such as seafloor spreading, or plate collision followed by erosion – transport residual mantle peridotite to the Earth's surface. These processes create a huge, near-surface reservoir of potential energy. In turn, this chemical potential drives retrograde metamorphism. Peridotite alteration plays an essential role in controlling the rheology of oceanic plates (Escartin et al., 1997) and subduction zones (Hilairet and Reynard, 2009), causes forearc uplift (Stern and Smoot, 1998), and fluxes arc magmatism (Ulmer and Trommsdorff, 1995). It plays a significant role in the geochemical water and carbon cycles (Hacker, 2008; Kelemen, et al., 2011). It produces some of the most reduced fluids on the surface of the Earth (Frost and Beard, 2007), and generates steep compositional gradients that are exploited by chemosynthetic organisms (Brazelton et al., 2010).

* Corresponding author. Tel.: +1 845 365 8728; mobile: +1 508 274 8631; fax: +1 845 365 8155.
E-mail addresses: peterk@LDEO.columbia.edu (P.B. Kelemen), greg_hirth@brown.edu (G. Hirth).

0012-821X/$ - see front matter © 2012 Elsevier B.V. All rights reserved.
http://dx.doi.org/10.1016/j.epsl.2012.06.018

It creates ideal conditions (low partial pressure of O_2, reduced carbon species such as CO and CH_4 in aqueous solutions, stable FeNi metal catalysts) for abiotic synthesis of organic compounds (McCollom et al., 2010), and has been invoked as an essential ingredient in the origin of life (McCollom, 2007).

Enhanced peridotite carbonation could play a significant role in CO_2 storage (Seifritz, 1990), or even a practical and inexpensive route to geological CO_2 capture (Kelemen et al., 2011; Kelemen and Matter, 2008). Studies of the mechanisms that form fractures during retrograde metamorphism of olivine (Jamtveit et al., 2008; MacDonald and Fyfe, 1985; Rudge et al., 2010) may also yield key insights into engineered creation of fracture systems for geothermal power and extraction of unconventional hydrocarbon resources.

Hydration of end-member, Mg-olivine (forsterite) can take place via the reaction:

$$2Mg_2SiO_4 + 3H_2O = Mg_3Si_2O_5(OH)_4 + Mg(OH)_2$$
$$\text{olivine} + \text{aqueous fluid} = \text{serpentine} + \text{brucite} \quad \text{(R1)}$$

Carbonation of olivine can occur via the simplified reaction:

$$Mg_2SiO_4 + 2CO_2 = 2MgCO_3 + SiO_2$$
$$\text{olivine} + CO_2 \text{ in fluid} = \text{magnesite} + \text{quartz} \quad \text{(R2)}$$

Combined hydration and carbonation can take place via a large variety of processes, e.g.,

$$2Mg_2SiO_4 + 2H_2O + CO_2 = Mg_3Si_2O_5(OH)_4 + MgCO_3$$
$$\text{olivine} + \text{aqueous fluid} + \text{dissolved } CO_2 \text{ in fluid} = \text{serpentine} + \text{magnesite} \quad \text{(R3)}$$

$$4Mg_2SiO_4 + H_2O + 5CO_2 = Mg_3Si_4O_{10}(OH)_2 + 5MgCO_3$$
$$\text{olivine} + \text{aqueous fluid} + \text{dissolved } CO_2 \text{ in fluid} = \text{talc} + \text{magnesite} \quad \text{(R4)}$$

These reactions can take on infinite variety when other naturally available components – such as Fe, Ca, the solid mineral pyroxene, or aqueous SiO_2 – are included. As written, Reactions (R1)–(R4) consume fluid components, increase the solid mass, and reduce the solid density. The molar ratio of solid/fluid reactants is 0.5 for Reaction (R2), and 0.67 for Reactions (R1), (R3) and (R4). These reactions increase the solid volume by 40–50% relative to the initial solid volume.

2. Fluid transport during retrograde metamorphism

It is often stated that negative feedbacks cause retrograde metamorphism to be self-limiting. Indeed, the common presence of rock outcrops recording high temperature and pressure phase equilibria attests to the selective operation of retrograde processes. Several negative feedbacks may be responsible for this. (1) In igneous and high-grade metamorphic rocks, fluid porosity and permeability may be negligibly small, so retrograde processes are fluid supply-limited. (2) Fluids enhance diffusion and so act as catalysts for recystallization. Prograde reactions produce fluids, in a positive feedback, while retrograde reactions may consume available fluid before recrystallization is complete. (3) Under some circumstances retrograde reactions may increase the solid volume, because they add mass to the solid rock, and because the hydrated and carbonated solid products have lower densities than the solid reactants.

Fluid–rock reactions that increase the solid volume may fill porosity, reduce permeability, and armor solid reactants with reaction rims (Aharonov et al., 1998). Decreasing permeability with reaction progress has been observed for hydration and carbonation of basalt (Becker and Davis, 2003). As a result of such observations, it is commonly assumed that peridotite hydration reduces permeability and limits alteration (Emmanuel and Berkowitz, 2006; Xu et al., 2004). Chizmeshya et al. (2007) observed a "passivating," SiO_2-rich reaction rim on olivine surfaces, formed during dissolution coupled with crystallization of magnesite+quartz. Perhaps for a similar reason, Martin and Fyfe (1970) observed experimental serpentinization rates decreasing with time, and O'Connor et al. (2004) observed a $\sim 3\times$ decrease in the rate between 26% and 93% olivine carbonation (Supplementary Fig. S4 in Kelemen et al., 2011).

Despite these potentially self-limiting, negative feedbacks, retrograde metamorphism of olivine commonly proceeds to completion. 100% hydrated peridotites, known as serpentinites, are well known. Less familiar, but of increasing scientific interest, are "listvenites", 100% carbonated peridotites composed of magnesite+quartz. Two end-member explanations for complete hydration and/or carbonation have been offered.

(1) As discussed in more detail in Sections 3 and 4.3, many metamorphic petrologists consider that retrograde replacement reactions occur at constant volume, in which expansion due to decreasing solid density is balanced by dissolution and export of chemical components in a fluid. In principle, such a constant volume process could preserve porosity, permeability and even reactive surface area. However, with notable exceptions, most studies of serpentinites, and our work on listvenites in Oman, suggest that in many cases alteration was nearly isochemical except for addition of H_2O and/or CO_2 (e.g., Coleman and Keith, 1971).

(2) MacDonald and Fyfe (1985) proposed that increasing stress due to volume expansion in an elastically confined volume causes fractures, which in turn increase or maintain permeability and reactive surface area, in a positive feedback mechanism that allows retrograde reactions like serpentinization to proceed to completion. This idea has been further investigated and quantified for serpentinization (Evans, 2004; Iyer, et al., 2008; Jamtveit et al., 2008; O'Hanley, 1992), olivine carbonation (Kelemen et al., 2011; Kelemen and Matter, 2008; Rudge et al., 2010), and weathering (Fletcher et al., 2006; Jamtveit et al., 2011; Royne et al., 2009). Similarly, Jamtveit et al. (2000) and Malthe-Sorenssen et al. (2006) explored the idea that solid volume decrease could lead to fracture formation.

Microstructural observations lend support to the hypothesis of MacDonald and Fyfe (1985). The ubiquitous presence of dense fracture networks that host serpentine veins in partially serpentinized peridotite, with ~10- to 100-micron spacing, lends credence to the idea that serpentinization and cracking are coeval. Without the presence of serpentine "glue" along these fracture networks, the host would be a powder rather than a rock. Furthermore, it is common to observe several generations of cross-cutting serpentine veins, which indicate repeated cycles of hierarchical fracturing followed by hydration (Iyer et al., 2008). Similarly, listvenites have brecciated textures in their outcrops and dense, hierarchical fracture networks extending to microscopic scales, filled by synkinematic carbonate and quartz veins. Cross-cutting relationships in partially carbonated peridotites indicate coeval carbonate crystallization and fracture (Fig. 8 in Kelemen et al., 2011). Also, geochronological data (^{14}C, U-series) show that permeability is maintained over tens of thousands of years in water-peridotite systems undergoing carbonation and serpentinization, both in Oman (Kelemen et al., 2011; Kelemen and Matter, 2008) and in the Lost City hydrothermal vent field along the Mid-Atlantic Ridge (Früh-Green et al., 2003; Ludwig, et al., 2011).

3. Crystallization pressure

In open systems undergoing metamorphism, the fluid porosity is restricted to cracks and/or small grain boundary pores. Despite the small instantaneous fluid–rock ratio, fluid flow through the porous network can lead to high, time-integrated fluid–rock ratios. Under these circumstances, the changes of the fluid volume within a given rock – due to fluid consumption or evolution by fluid-solid reactions – are small. By contrast, solid volume increase, via addition of fluid components to solid minerals and reduction of the density of solid products compared to reactants, potentially leads to permanent and significant changes in rock volume.

In calling upon reaction-driven cracking in response to solid volume expansion, the papers enumerated in the previous section invoked a long tradition of research on the "force of crystallization". Early and insightful work on this was reviewed by Lindgren (1912), who wrote that "the prevailing view in the earlier days of the science of ore deposits was that the growing crystal had by means of its 'force of crystallization' pushed apart the surrounding mass". Becker and Day (1905) demonstrated that confined crystals of "alum" ($KAl(SO_4)_2 \cdot 12H_2O$), growing from a supersaturated aqueous solution, could lift considerable weights, and wrote "that the linear force thus exerted is of the order of magnitude of the breaking strength of the crystal and therefore a geologic force of considerable magnitude and importance". Similarly, Taber (1929) showed that growing ice crystals could lift substantial loads.

Many papers have followed, with those most relevant to our study focusing on replacement processes in earth science. Although some geologists emphasized evidence for viscous deformation of the host rock during crystallization of a new phase (e.g., Misch, 1971; Yardley, 1974), consensus gradually arose among metamorphic petrologists that most rocks should be considered very nearly rigid, and therefore that the pressure during crystallization of a new phase, elastically deforming the host rock, would gradually increase until pressure dependent solubility rose sufficiently to drive dissolution of the host phase at the same volumetric rate as crystallization of the product phase (e.g., Carmichael, 1986). Exceptions, in which the host rock could undergo irreversible deformation via viscous flow or fracture, were mentioned but given little quantitative attention until the study of Fletcher and Merino (2001).

Strangely, outside the field of metamorphic petrology, a parallel literature has developed on irreversible deformation via dilatant cracking, driven by volume expansion due to formation of a new phase from fluid in pore space, with increasing solid mass and/or decreasing density, and without appreciable dissolution of the host rock. This literature focused on "salt weathering" (e.g., reviews and recent experiments by Scherer (2004) and Steiger, 2005). Related papers focus on fracture due to the density decrease during maturation of hydrocarbons (e.g., Berg and Gangi, 1999). Fletcher et al. (2006), Royne et al. (2009) and Jamtveit et al. (2011) provide recent applications of this concept to spheroidal weathering.

Cracking due to salt crystallization in pore space is most likely during rapid precipitation because increasing stress in the host rock competes with slow relaxation mechanisms such as dislocation creep within growing crystals. For example, in experiments on crystallization of Na-sulfate salts in porous limestone, rapid crystallization caused fractures, whereas slow crystallization did not (Espinosa Marzal and Scherer, 2008). The stress required to fracture the unconfined limestone blocks at atmospheric pressure is $\sim$1 MPa. Salts have low viscosity (Spiers et al., 1990), and 1-MPa stresses relax in microseconds to minutes for 1–100-μm salt crystals. Thus, increasing stress due to salt crystallization in pore space had to take place in seconds to minutes to produce fracture rather than viscous flow of salt.

Cracking may also be favored when fluid flow takes place periodically followed by rapid evaporation, as may be common in arid areas subject to occasionally heavy rainfall. As noted by Scherer (2004), rapid evaporation of isolated fluid pockets in pore space drives increasing solute concentrations and potentially extreme supersaturation. This, in turn, could produce very high pressures of crystallization, as in most experiments demonstrating the process of salt weathering (e.g., Noiriel et al., 2010).

Quantitative analyses of experiments (Correns, 1949; Correns and Steinborn, 1939) demonstrated that crystal growth from a fluid in pore space, driven by surface energy and diffusion of components in a nanofilm along the contact between a growing crystal and its host, leads to local stresses in excess of the confining pressure, proportional to the extent of supersaturation of the growing mineral. In the simplest formulation, the "crystallization pressure" is given by

$$P' = \frac{RT}{V_m} \ln\left(\frac{c}{c_0}\right) \tag{E1}$$

where R is the gas constant, T is the temperature in Kelvin, V_m is the molar volume of the growing crystalline phase, c is the concentration of a solute, c_0 is the equilibrium concentration at which fluid is saturated in the growing crystalline phase, and P' is a localized excess pressure or "overpressure", in excess of the confining pressure. Elsewhere in this paper, following previous work on this topic, we have also referred to P' as "crystallization pressure". Increasing P' around a growing crystal creates a pressure gradient, and thus a differential stress that can lead to fracture. As an example, Steiger (2005) calculates crystallization pressures of tens to more than one hundred MPa for crystallization of supersaturated NaCl in pore space.

Steiger (2005) notes that the formulation using c/c_0 is correct only for ideal solutions in which a growing crystal forms via precipitation of a single fluid component. Given that the "reaction quotient", Q, is the product of activities of products divided by the product of activities of reactants, whereas the "equilibrium constant", K, is the reaction quotient for a system in equilibrium, c/c_0 should be replaced with the reaction quotient for a crystallization reaction divided by the equilibrium constant for that reaction, Q_{precip}/K_{precip}. For a reaction such as dissolution of magnesite in water, $MgCO_{3(s)} = Mg^{++}_{(aq)} + CO^{2-}_{3(aq)}$, the saturation state Ω is the ratio Q_{diss}/K_{diss}, which in turn is equal to K_{precip}/Q_{precip} for $Mg^{++}_{(aq)} + CO^{2-}_{3(aq)} = MgCO_{3(s)}$, so an improved equation for overpressure resulting from a crystallization reaction is

$$P' = -\frac{RT}{V_m} \ln\left(\frac{Q_{precip}}{K_{precip}}\right) = \frac{RT}{V_m} \ln(\Omega) \tag{E2}$$

For pure magnesite, $a_{MgCO_3} = 1$, and

$$\Omega = Q_{diss}/K_{diss} = \frac{a_{Mg^{++}} a_{CO_3^{2-}}}{a_{MgCO_3}} / K_{diss,MgCO_3} = \frac{a_{Mg^{++}} a_{CO_3^{2-}}}{K_{diss,MgCO_3}} \tag{E3}$$

Recent studies of (notoriously sluggish) magnesite crystallization kinetics (Hänchen et al., 2008; Saldi et al., 2009) found that Ω can exceed 100 at temperatures up to 120 °C. Under these conditions, Eq. (E2) yields crystallization pressures greater than 500 MPa. Such overpressures, and resulting differential stresses, are more than sufficient to fracture crustal rocks.

In geologic applications, we commonly do not know the composition of the fluid that was involved in a mineral precipitation reaction at some time in the past. However, we can estimate the maximum crystallization pressures that could arise during precipitation of a mineral from an oversaturated fluid, or due to spontaneous, retrograde olivine hydration and carbonation reactions, using the Gibbs Free Energy of the reactions. Using the standard-state Gibbs Free Energy for a reaction, $\Delta G^0_r = -RT \ln(K)$, the Gibbs Free Energy change for a precipitation reaction at

constant temperature and confining pressure can be expressed as

$$\Delta G_r = -RT\ln(K_{precip}) + RT\ln(Q_{precip}) = RT\ln\left(\frac{Q_{precip}}{K_{precip}}\right) = -RT\ln(\Omega) \tag{E4}$$

and thus

$$P' = -\frac{\Delta G_r}{\Delta V_s} \tag{E5}$$

where ΔV_s is the difference in volume between the solid products and the solid reactants (Kelemen et al., 2011) and $\Omega = K_{precip}/Q_{precip}$ for retrograde reactions such as Reactions (R1)–(R4) proceeding from left to right as given in Section 1, above. Eq. (E5) is valid for reactions involving solid reactants, such olivine serpentinization and carbonation, as well as for reactions that only involve precipitation of solid products. When a process only involves crystallization of a new phase from solute in the fluid, $\Delta V_s = V_m$ as in Eqs. (E1) and (E2). More generally, ΔV_s includes the volume decrease due to solid reactant (olivine) dissolution as well as the volume increase due to precipitation of solid products (serpentine, brucite, magnesite and quartz in Reactions (R1)–(R4)).

Following, e.g., Correns, Steiger, and Fletcher and Merino, we assume that changes in the volume of the fluid phase are negligible in rocks with low porosity (low instantaneous fluid/rock ratio) that are constantly supplied with fluid flowing through the pores (high time-integrated fluid rock ratio). Since the Gibbs Free Energy of reaction is the available chemical potential energy at constant temperature and pressure, this expression provides an estimate of the crystallization pressure that can be generated under these conditions.

Upon consideration of Eqs. (E1)–(E5), several points become evident. Workers since Correns have implicitly assumed that almost all of the chemical potential energy inherent in oversaturated fluids, when released by crystallization of the saturated phase, will be converted into overpressure or differential stress. However, thermal diffusion of energy released by exothermic crystallization reactions, maintaining constant temperature for example, could reduce the energy available for mechanical work. Also, entropy changes resulting from reaction may consume or contribute to the energy available to generate overpressure and cause deformation. Generally, for crystallization from fluid, and for retrograde hydration and carbonation of olivine, the entropy change is negative, reducing the energy available to generate crystallization pressure. Thus, Eq. (E5) yields an upper bound on the energy available to produce overpressure at constant temperature and pressure.

Under some circumstances, the available chemical potential energy might be better characterized using the Helmholtz Free Energy, valid for conditions of constant temperature and volume. The Helmholtz Free Energy of reaction is related to the Gibbs Free Energy via

$$\Delta F_r = \Delta G_r - P\Delta V_r \tag{E5a}$$

where P is the confining pressure and ΔV_r is the molar volume of the reaction products minus reactants, including fluid volumes. Thus for the case of negligible instantaneous fluid volume change (small and/or constant porosity), the maximum overpressure that can be produced by the available chemical potential energy might be expressed as

$$P' = -\frac{\Delta F_r}{\Delta V_s} = -\frac{\Delta G_r}{\Delta V_s} + \frac{P\Delta V_r}{\Delta V_s}. \tag{E5b}$$

For precipitation of new minerals from pore fluid, and for the hydration and carbonation of olivine considered in the next section, ΔV_r is negative while ΔV_s is positive. For such reactions, under conditions of constant temperature and volume, the chemical potential energy available to produce overpressure may decrease with increasing confining pressure.

4. Stresses arising from retrograde replacement of olivine

Igneous rocks called troctolites are composed mainly of the minerals olivine and plagioclase. In typical troctolites, rounded olivine crystals are surrounded by interstitial plagioclase. Hatch et al. (1949), Evans (2004), Jamtveit et al. (2008) and Beard et al. (2009) emphasize textural evidence for reaction-driven cracking in troctolite samples, in which partial serpentinization of olivine has shattered surrounding plagioclase crystals. In this paper, we use their observations to estimate the stress due to volume expansion of serpentinization within an elastic medium, and to place bounds on the stress responsible for plagioclase fracture.

We take three approaches to estimating the stresses arising from retrograde replacement of olivine, focusing on end-member Reactions (R1) and (R2). First, we estimate the available chemical potential energy in terms of crystallization pressure, P', using Eq. (E5). Local gradients in P' give rise to differential stresses with similar magnitude. Our second and third methods rely on microstructural observations. In the second method, we use the observation that olivine serpentinization drives cracking in surrounding plagioclase crystals, together with an estimate of the surface energy created by this fracture process. In the third method, we estimate the stress that would be generated by elastic deformation of surrounding plagioclase crystals by olivine hydration, if cracking did not occur and there was no dissolution of plagioclase.

4.1. Crystallization pressure from chemical potential

When fluid comes into contact with olivine, there is a chemical potential driving the reactions to form serpentine and/or magnesite, together with brucite, quartz and other minerals. At constant temperature and pressure, this chemical potential can be approximated by the Gibbs Free Energy change due to Reactions (R1) and (R2). The Gibbs Free Energies for these reactions are illustrated in Fig. 1. Readers should note that the thermodynamic properties for the minerals and fluids involved are poorly known (e.g., Evans, 2004). Estimates of the uncertainties can be found in the caption of Fig. 1.

Eq. (E5) yields upper bounds for crystallization pressures illustrated in Fig. 2. Where these crystallization pressures develop locally around growing crystals, they will lead to gradients in pressure, and thus to differential stress. Although they are approximate – for chemically simple systems at constant temperature, involving phases whose thermodynamic properties are not well known – these illustrative calculations show that there is more than enough energy to fracture rocks when olivine undergoes serpentinization and/or carbonation. Uncertainties are shown graphically in Fig. 2.

4.2. Stress estimated from fracture energy density

Microcracks form from conversion of strain energy, u_e, to surface energy, γ (Lawn and Wilshaw, 1975). The strain energy density is $u_\varepsilon = \frac{1}{2}\sigma\varepsilon_e$, where σ is differential stress and ε_e is elastic strain. Because the elastic strain is a function of stress and Young's modulus, E, $\varepsilon_e = \sigma/E$ so that the strain energy density is

$$u_\varepsilon = \frac{\sigma^2}{2E} \tag{E6}$$

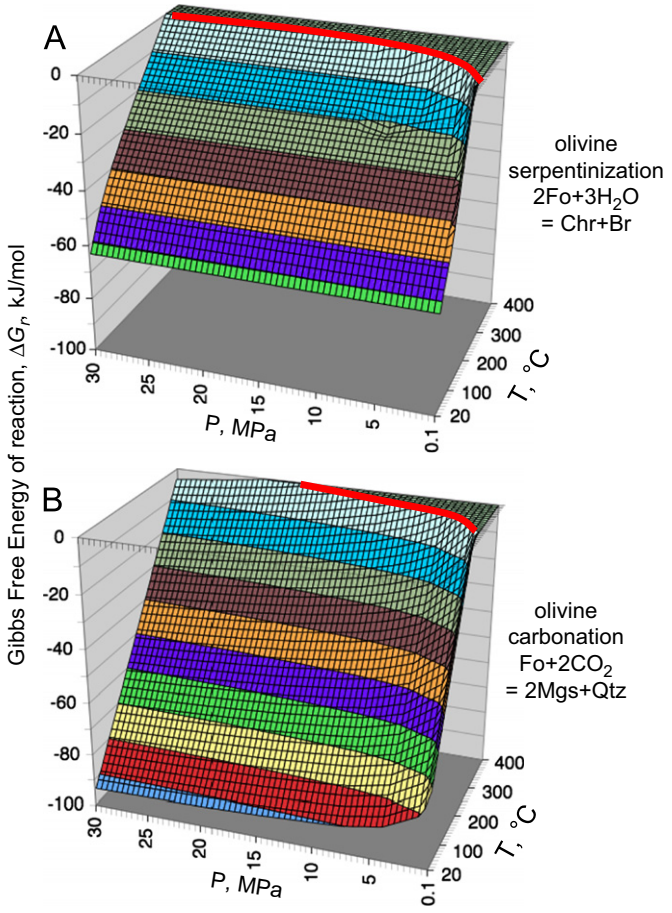

Fig. 1. Gibbs Free Energies of reaction in kilojoules per mole for olivine serpentinization (Reaction (R1) in text, panel A in figure) and carbonation (Reaction (R2) in text, panel B in figure) in the systems MgO–SiO_2–H_2O and MgO–SiO_2–CO_2, as a function of temperature and confining pressure. These values were calculated using internally consistent thermodynamic data for Mg end-member minerals forsterite (Mg_2SiO_4 olivine, Fo), chrysotile (low temperature serpentine polymorph, $Mg_3Si_2O_5(OH)_4$, Chr), brucite ($Mg(OH)_2$, Br), magnesite ($MgCO_3$, Mgs) and quartz (SiO_2, Qtz) from Gottschalk (1997) and the equations of state for pure H_2O (panel A) and pure CO_2 (panel B) gases from Duan et al. (1992), with fluid pressure equal to the confining pressure.

The uncertainty for panel A is small compared to the magnitude of variation of the Gibbs Free Energy of reaction. For example, it is less than ± 3 kJ/mol at 200 °C, 100 MPa, calculated using 2σ uncertainties from Gottschalk (plus Holland and Powell (1990) for the uncertainty of H_2O enthalpy), and $\pm 10\%$ for the fugacity of H_2O from Fig. (8) and (9) of Duan et al. (1992). The small kink in the free energy surface at ~250 °C, 10 MPa reflects variation in H_2O fugacity near the boiling curve. The uncertainty for panel B is also small compared to the variation in Free Energy. For example, it is less than ± 2.5 kJ/mol at 200 °C, 100 MPa, using 2σ uncertainties from Gottschalk (plus Holland and Powell (1990) for CO_2 enthalpy), and $\pm 5\%$ for the fugacity of CO_2 from Fig. (5) and (6) of Duan et al. (1992). Another way to estimate the uncertainty of these values is to compare results calculated with different, internally consistent thermodynamic data sets. For example, at 200 °C and 100 MPa, the calculated Gibbs Free Energy of reaction is −23.8, −25.3 and −25.5 kJ/mol for olivine serpentinization (panel A), and −43.2, 47.2 and −48.6 kJ/mol for olivine carbonation (panel B), using the data of Gottschalk (1997), Holland and Powell (1990) and Berman (1988) respectively, all with the Duan et al. (1992) equations of state.

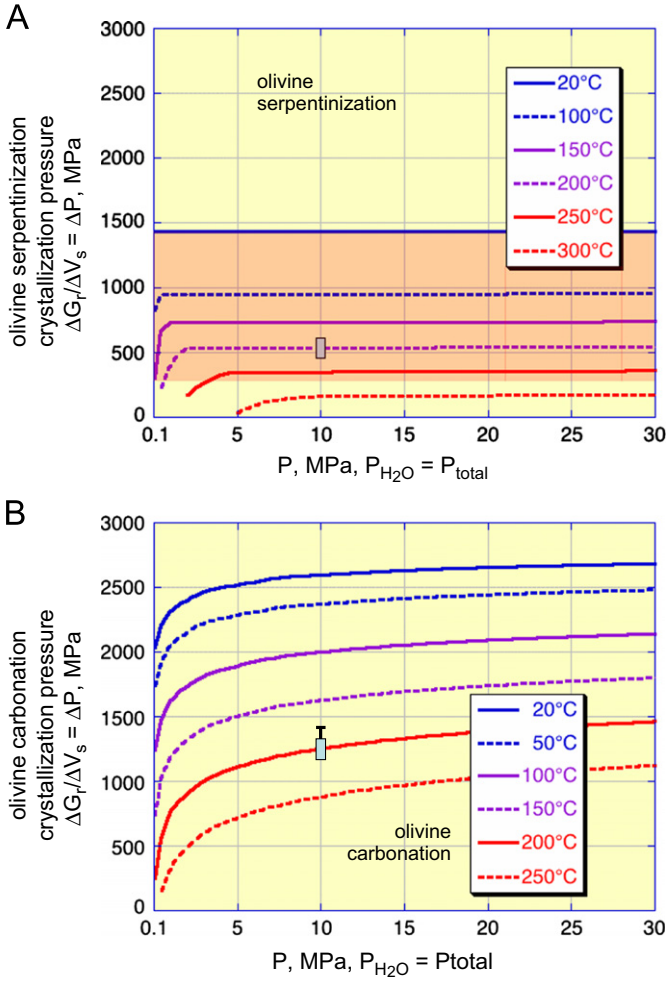

Fig. 2. Isopleths of upper bound crystallization pressures in MPa for olivine serpentinization (Reaction (R1) in text, panel A in figure) and carbonation (Reaction R2 in text, panel B in figure), as a function of temperature and confining pressure. The red shaded area in panel A illustrates the region that simultaneously satisfies the upper bound constraints shown here and the lower bound constraints on stress due to olivine serpentinization from Eq. (E12), at a temperature greater than 20 °C. Crystallization pressures exceeding ~100–500 MPa, as indicated by the structural data discussed in Section 4.2, arise from olivine serpentinization at a confining pressure greater than a few 10's of MPa when the temperature is less than ~325–175 °C.

To calculate the upper bound crystallization pressures illustrated as isopleths in this figure, we used Eq. (E5), with ΔG_r calculated from the internally consistent data set of Gottschalk (1997), as in Fig. 1, with ΔV_s of 4.4×10^{-5} m^3/mol for (A) and 3.5×10^{-5} m^3/mol for (B). Uncertainties in Gibbs Free Energies calculated from the Gottschalk (1997) and Duan et al. (1992) thermodynamic data, estimated as described in the caption of Fig. 1, were recalculated as crystallization pressures, and are shown as gray bars at 200 °C and 100 MPa. As described in the caption of Fig. 1, the thermodynamic data of Holland and Powell (1990) and Berman (1988) yield significantly higher values for the crystallization pressure of olivine carbonation at these conditions, as indicated with a black line extending above the gray bar in panel B.

The surface energy density u_γ created by new cracks in plagioclase is

$$u_\gamma = 2\gamma \frac{\Sigma A_c}{V_p} \text{ or in two dimensions, } u_\gamma = 2\gamma \frac{\Sigma L_c}{A_p} \tag{E7}$$

where L_c is the crack length (the spacing of olivine crystals in the plagioclase matrix), A_c is the surface area of cracks, and V_p and A_p are the volume and area of plagioclase hosting the cracks, so that $\Sigma A_c/V_p$ and $\Sigma L_c/A_p$ are crack densities in three and two dimensions.

In the partially serpentinized troctolites, the strain energy density must have been greater than the surface energy of the new cracks

$$u_\varepsilon > u_\gamma \tag{E8}$$

so by substitution into Eq. (E6), $\sigma^2 = 2u_\varepsilon E > 2u_\gamma E$, and

$$\sigma > \sqrt{4E\gamma \frac{\Sigma L_c}{A_p}}. \tag{E9}$$

Young's modulus and surface energy are known, and we can measure crack densities from the microstructure of serpentinized olivine–plagioclase rocks as follows.

Fig. 3 provides illustrations of cracked, rectangular plagioclase grains between two olivine grains with serpentine veins replacing the olivine at regular intervals. The spacing between the serpentine veins in olivine, W, is about 500 μm in the images published by Hatch et al. (1949), Evans (2004), Jamtveit et al. (2008) and Beard et al. (2009). The serpentine veins are about 20 μm wide. The crack spacing in plagioclase between the olivine grains averages about 6 μm (Fig. 2A in Jamtveit et al. (2008)). There are also cracks along the olivine–plagioclase grain boundaries. The width of the plagioclase grains between the olivine grains is about 3 mm.

A characteristic area in the plagioclase with width W is $A_p = WL_c$. The sum of the lengths of cracks in this area is

$$\Sigma L_c = WL_c/w + 2W \sim WL_c/w \tag{E10}$$

so that

$$\Sigma L_c/A_p = \Sigma A_c/V_p = 1/w. \tag{E11}$$

For E in plagioclase of $\sim 10^{11}$ kg/ms^2, γ of ~ 1 J/m^2, and $1/w$ $\sim 2 \times 10^5$ m^{-1}, this yields

$$\sigma > \sqrt{\frac{4E\gamma}{w}} = 260 \text{ MPa}(+260, -130 \text{ MPa}). \tag{E12}$$

Again, as for the thermodynamic calculations in Section 4.1, readers should keep in mind that this is an illustrative calculation of the lower bound for strain energy density in some troctolite samples. In this calculation we have used approximate, average values for naturally variable crack spacing and length, together with approximate values for surface energy of cracks and Young's modulus in plagioclase. For example, experimentally-derived surface energies of quartz, plagioclase and potassium feldspars are similar, with plus or minus a factor of four variation from 0.25 to 4 J/m^2 (Atkinson and Avdis, 1980; Brace and Walsh, 1962; Tapponnier and Brace, 1976; Wong, 1982). This corresponds to the uncertainty of plus or minus a factor of two in the results from Eq. (E12), above.

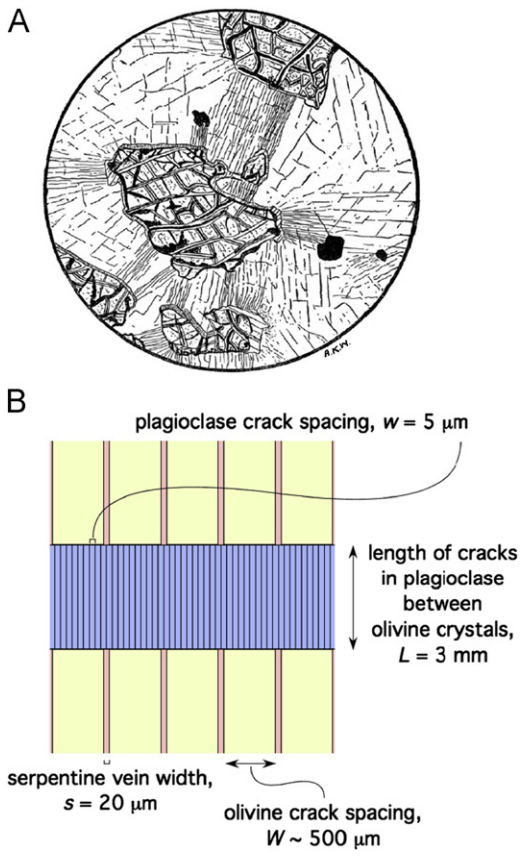

Fig. 3. (A) Sketch of fractured plagioclase grains between partially serpentinized olivine crystals (stippled) with iron-oxides (black) from Hatch et al. (1949), as reproduced by Evans (2004). Field of view approximately 6 mm. (B) Schematic interpretation of the textures documented by Hatch et al. (1949), Evans (2004), Jamtveit et al. (2008) and Beard et al. (2009).

Combining the calculations in Sections 4.1 and 4.2, and their uncertainties, we can infer from Fig. 2 that the stress due to volume expansion during olivine serpentinization at depths of a few kilometers or more would have been generated at a temperature less than about 275 $(+50, -100)$ °C. This constraint is reasonable for alteration of troctolites, suggesting that our calculations are approximately correct. Note that we have assumed that all the cracks between a given pair of olivine crystals formed during the same event, and not one crack at a time. This seems likely. If, instead, crack formation were sequential, dilation along a single crack could have accommodated most of the subsequent volume expansion and few additional cracks would have formed.

4.3. Stress arising from elastic strain in plagioclase

If there were no cracks across the plagioclase crystals, and if volume expansion in olivine on both sides of the plagioclase grain in Fig. 3 were the same, combined elastic deformation within the plagioclase, slip on the plagioclase–olivine grain boundaries, and viscous deformation, would be equivalent to the volume expansion during serpentinization. If H_2O is added to olivine, and no chemical components are removed from solution, the change in solid volume during complete serpentinization via Reaction (R1) is 40–50% (depending on the amount of iron in the olivine, and the proportion of iron in oxide minerals produced during serpentinization). The elastic strain in the plagioclase grain is

$$\varepsilon_e \leq \Delta V_s s/W \tag{E13}$$

where s is the width of serpentinized fractures in olivine, and the resulting stress is

$$\sigma = E\varepsilon_e \leq E\Delta V_s s/W \sim 2000 \text{ MPa}. \tag{E14}$$

This is clearly much larger than the fracture strength of crustal rocks, and much greater than the stress calculated from the observed crack spacing in plagioclase (Eq. (E12)). There are three ways to account for this large difference:

(a) Once plagioclase is cracked, with fluid in the cracks lowering the effective pressure, its elastic moduli may be reduced substantially (Fig. 2 in Walsh (1965)). If Young's modulus were reduced by a factor of ~8, as is possible, Eq. (E14) would yield a stress ≤ 250 MPa, consistent with the result from Eq. (E12).

(b) Volume change due to serpentinization could have been largely accommodated by irreversible dilation of the microcracks. In a given width W, the total displacement $\Delta V_s s = 10$ μm. Assuming that the stress due to serpentinization was in the range of 130–520 MPa (from Eq. (E12)), 94–54% of the displacement must have been accommodated by irreversible deformation. Given that the number of cracks in plagioclase in the width W is $w/W \sim 100$, this would entail ~100–50 nm of dilation on each crack, in keeping with observed crack widths in crystalline rocks (Hadley, 1976; Sprunt and Brace, 1974). Backscattered electron images of the cracks in plagioclase (Jamtveit et al., 2008) show much wider apertures, filled with alteration minerals such as zeolites, but these probably

widened during decompression following serpentinization, during subsequent uplift and erosion.

(c) Some of the expansion due to serpentinization could have been accommodated by dissolution of olivine or plagioclase, with export of excess material out of the rock volume as proposed, for example, by Fletcher and Merino (2001). However, their analysis lacks several aspects of the problem considered here. Most importantly, they do not consider disequilibrium between fluid and the host phase that drives reactions to form a newly crystallizing phase.

Dewers and Ortoleva (1990) and Fletcher and Merino (2001) derive expressions very similar to (E1)–(E5), but consider them to yield an upper bound on crystallization pressure, applicable under conditions of constant solid volume when the volumetric rate of crystallization of the product solid phase in a free fluid is much larger than the rate of dissolution of the host phase in a free fluid. They show that under some conditions this is a transient condition followed by a steady state in which precipitation and dissolution rates are identical.

Following the analysis of Fletcher and Merino (2001), Section 4, using $\Omega=2$ as they do, and kinetic data compiled by Palandri and Kharaka (2004), we would infer crystallization pressures of 20–80 MPa for the steady state in which volumetric plagioclase and/or olivine dissolution rates would be equal to the serpentine precipitation rate. However, from the Gibbs Free Energy of the reactions, and Eq. (E4), we find $\Omega\sim10^7$ for olivine serpentinization and carbonation, because olivine is so far from equilibrium with aqueous fluids under near-surface conditions. The steady state crystallization pressure of Fletcher and Merino, when dissolution of the host phase occurs at the same rate as precipitation of the new phase, is proportional to $\ln(\Omega)$, and thus would be twenty times larger for $\Omega\sim10^7$ rather than $\Omega=2$, yielding steady state crystallization pressures in the range of 400–1600 MPa. These pressures are greater than the fracture strength of plagioclase in the crust. As a result, we infer that plagioclase hosting serpentinizing olivine cracks and deforms along the newly formed fractures, and thus does not reach the steady state crystallization pressure for constant volume replacement invoked by Fletcher and Merino (2001).

5. Feedback processes during retrograde metamorphism

From the perspective of rock mechanics, there are at least three possible mechanisms to accommodate decreasing solid phase density, and possibly increasing solid mass, during retrograde replacement reactions.

(a) Pressure solution in response to small stress gradients, combined with
  (a1) filling of pore space with newly precipitated solid phases and/or
  (a2) export of components to some other site, can remove most or all of the excess solid volume.

(b) Increasing differential stress – driven by elastic strain in response to local volume changes – can cause viscous deformation of the solid phases (e.g., by dislocation creep). This can occur via
  (b1) solid-state flow of the newly formed phases, which may displace fluid to take on the shape of pore space, or via
  (b2) deformation of the pre-existing host phases, either into pore space or by an irreversible increase in the rock volume. Near the surface, b2 could take the form of an increase in elevation.

(c) Dilatant fracture and expansion – for example, an increase in surface elevation – of the rock volume in response to increasing differential stress, as in salt-weathering.

In the previous sections of this paper, we focus on (c). However, it would be valuable to have a "phase diagram" characterizing the physical conditions required for each mechanism, and delineating the fields within which a particular mechanism is likely to prevail. It is beyond the scope of this paper to complete such a process, but in this section we attempt a beginning.

In general, interconnected fractures containing aqueous fluid at hydrostatic pressure dominate the rheology of the upper 10 km in stable plates (Zoback and Townend, 2001). These portions of the crust deform irreversibly by sliding on fractures. As we have seen, stress arising from serpentinization of olivine in several examples was of the order of 300 MPa, which is the frictional yield stress for the crust in compression at approximately 9 km depth. It is evident that volume expansion due to serpentinization continued to this stress, and the conditions for constant volume replacement (Fletcher and Merino, 2001) were not attained.

Given that serpentinization and carbonation of olivine at low temperature is sufficient to generate crystallization pressures exceeding 1 GPa, greater than the frictional failure stress at any depth where serpentine and/or Mg-carbonates are stable on a normal geotherm (away from subduction zones), we believe that the criteria for constant volume replacement may never be attained for retrograde metamorphism of olivine, which – instead – will always drive irreversible deformation of the host rock. However, stresses sufficient for fracture may not always arise. If viscous relaxation is more rapid than the stress increase due to reaction-driven increase in the solid volume, the system may expand irreversibly without fracture.

Olivine hydration and carbonation become faster with increasing temperature due to increasing rates of diffusion within crystals and fluid, and increasing mass transfer across the mineral surface. Conversely, at a given fluid pressure, the chemical potential driving reaction decreases with increasing temperature (Fig. 1). The combination of these two effects leads to a maximum reaction rate at $\sim$260 °C for serpentinization, and $\sim$185 °C for carbonation (Martin and Fyfe, 1970; O'Connor et al., 2004). Given the high viscosity of host peridotite at these temperatures, reaction driven cracking is likely as long as fluid supply is rapid. However, at conditions where reaction is slow (lower temperature, higher temperature, limited fluid supply), viscous deformation of serpentine or carbonate reaction products might relax the stress generated by volume expansion.

The three mechanisms outlined here have different outcomes in terms of porosity, permeability, and reactive surface area, and therefore important feedbacks to the rate of retrograde metamorphic processes. Mechanisms (a) and (b) potentially lead to filling of pore space and armoring of reactive surfaces, and thus could involve negative feedbacks to reaction progress. In contrast, mechanism (c) could yield nearly constant or even increasing porosity, permeability and reactive surface area, positive feedback processes that may lead to 100% replacement of the host rock by retrograde metamorphic minerals.

6. Conclusions and implications

Natural examples of closely spaced fractures in host plagioclase, caused by volume expansion during serpentinization of olivine inclusions, indicate that stress arising from olivine serpentinization reached $\sim$300 MPa and was then limited by the

process of fracture formation, dilation and/or frictional sliding on these fractures, and – presumably – associated volume expansion in the host rock.

(1) The values of differential stress inferred from microstructures are in approximate agreement with thermodynamic estimates, and suggest that the methods used here could yield bounds on crystallization pressure for other retrograde reactions. In the absence of irreversible deformation of the host rock, by viscous flow or dilatant fracture, the stress arising from replacement of olivine by magnesite + quartz is likely to be substantially larger, at a given temperature, than the stress due to olivine serpentinization.

(2) Host rock viscosities are likely to be very high where serpentinization and carbonation rates are fastest, so that reaction-driven fracture, frictional sliding along these fractures, and subsequent increase in the rock volume are likely to result from retrograde metamorphism of olivine, limiting the stress generated by retrograde metamorphic reactions. In addition, increasing rock volume may often be accommodated by an increase in surface elevation, and/or by increased rates of surface erosion.

(3) Where initial permeability is sufficient to assure continuous supply of aqueous fluids, positive feedback between reaction-driven cracking, fluid supply, and reactive surface area is most likely to give rise to nearly 100% serpentinization or carbonation at the optimal temperatures for these reactions, ~260 and 185 °C, respectively. Ideally, engineered systems for in situ storage of CO_2, or for geological capture and storage of CO_2, should maintain a subsurface rock volume near 185 °C.

(4) Plate tectonic processes may be significantly influenced by stresses arising from retrograde metamorphism of olivine. Aside from effects on viscosity due to replacement of olivine by serpentine, talc, carbonate minerals and/or quartz, the differential stress due to retrograde replacement reactions could lead to tectonically significant deformation of host rocks. Regions composed of serpentinizing peridotite that have high initial porosity – for example in oceanic fracture zones and along normal faults at the outer rise near subduction zones – are likely to experience locally generated differential stresses equivalent to the fracture toughness and/or to the stress required for frictional sliding along fractures in altered peridotite. For example, these stresses could reach ~1 GPa at depths greater than ~20 km, perhaps contributing to bending and unbending of the shallow mantle section in subducting plates.

Acknowledgments

We would like to thank Bjørn Jamtveit and an anonymous reviewer, plus EPSL Editor Yanick Ricard, for constructive and helpful reviews. We are also grateful for informal advice and help from Bjørn Jamtveit, Lisa Streit, Dave Walker, George Scherer, Bernard Evans, Ray Fletcher, Enrico Bonatti, Reid Cooper, Ron Frost, Jim Beard and Marc Spiegelman. Kelemen's effort on this project was supported by NSF Research Grants EAR 0739010, EAR 0742368, and EAR 1049905, and by his Arthur D. Storke Chair at Columbia University. Hirth's effort was supported by NSF Research Grants EAR 0810188 and EAR 1049582.

References

Aharonov, E., Tenthory, E., Scholz, C.H., 1998. Precipitation sealing and diagenesis—2. Theoretical analysis. J. Geophys. Res. 103, 23969.

Atkinson, B.K., Avdis, V., 1980. Fracture-mechanics parameters of some rock-forming minerals determined using an indentation technique. Int. J. Rock Mech. Min. Sci. 17, 383–386.

Barnes, I., O'Neil, J.R., 1969. Relationship between fluids in some fresh alpine-type ultramafics and possible modern serpentinization, western United States. GSA Bull. 80, 1947–1960.

Beard, J.S., Frost, B.R., Fryer, P., McCaig, A., Searle, R., Ildefonse, B., Zinin, P., Sharma, S.K., 2009. Onset and progression of serpentinization and magnetite formation in olivine-rich troctolite from IODP Hole U1309D. J. Petrol. 50, 387–403.

Becker, G.F., Day, A.L., 1905. The linear force of growing crystals. Proc. Wash. Acad. Sci. 7, 283–288.

Becker, K., Davis, E., 2003. New evidence for age variation and scale effects of permeabilities of young oceanic crust from borehole thermal and pressure measurements. Earth Planet. Sci. Lett. 210, 499–508.

Berg, R.R., Gangi, A.F., 1999. Primary migration by oil-generation microfracturing in low-permeability source rocks: application to the Austin Chalk, Texas. AAPG Bull. 83, 727–756.

Berman, R.G., 1988. Internally-consistent thermodynamic data for minerals in the system Na_2O–K_2O–CaO–MgO–FeO–Fe_2O_3–Al_2O_3–SiO_2–TiO_2–H_2O–CO_2. J. Petrol. 29, 445–522.

Brace, W.F., Walsh, J.B., 1962. Some direct measurements of the surface energy of quartz and orthoclase. Am. Mineral. 47, 1111–1122.

Brazelton, W.J., Ludwig, K.A., M.L., S., Andreishcheva, E.N., Kelley, D.S., Shen, C.-C., Edwards, L., Baross, J.A., 2010. Archaea and bacteria with surprising microdiversity show shifts in dominance over 1000-year time scales in hydrothermal chimneys. Proc. Natl. Acad. Sci. USA 107, 1612–1617.

Carmichael, D.M., 1986. Induced stress and secondary mass transfer: thermodynamic basis for the tendency toward constant-volume constraint in diffusion metasomatism. In: Helgeson, H.C. (Ed.), Chemical Transport in Metasomatic Processes NATO ASI Series C, 218; 1986, pp. 237–264.

Chizmeshya, A.V.G., McKelvy, M.J., Squires, K., Carpenter, R.W., Béarat, H., 2007. DOE final Report 924162: A Novel Approach to Mineral Carbonation: Enhancing Carbonation While Avoiding Mineral Pretreatment Process Cost. Arizona State University, Tempe, AZ, 29 pp. plus appendices..

Coleman, R.G., Keith, T.E., 1971. A chemical study of serpentinization, Burro Mountain, California. J. Petrol. 12, 311–328.

Correns, C.W., 1949. Growth and dissolution of crystals under linear pressure. Discuss. Faraday Soc. 5, 267–271.

Correns, C.W., Steinborn, W., 1939. Experimente zur messung und erklärung der sogenannten kristallisationskraft. Z. Kristallogr. A 101, 117–133.

Dewers, T., Ortoleva, P., 1990. Force of crystallization during the growth of siliceous concretions. Geology 18, 204–207.

Duan, Z., Miller, N., Weare, J.H., 1992. An equation of state for the CH_4–CO_2–H_2O system: I. Pure systems from 0 to 1000 °C and 0 to 8000 bar. Geochim. Cosmochim. Acta 56, 2605–2617.

Emmanuel, S., Berkowitz, B., 2006. Suppression and stimulation of seafloor hydrothermal convection by exothermic mineral hydration. Earth Planet. Sci. Lett. 243, 657–668.

Escartin, J., Hirth, G., Evans, B., 1997. Effects of serpentinization on the lithospheric strength and the style of normal faulting at slow-spreading ridges. Earth Planet. Sci. Lett. 151, 181–189.

Espinosa Marzal, R.M., Scherer, G.W., 2008. Crystallization of sodium sulfate salts in limestone. Environ. Geol. 56, 605–621.

Evans, B.W., 1977. Metamorphism of alpine peridotite and serpentinite. Annu. Rev. Earth Planet. Sci. 5, 397–447.

Evans, B.W., 2004. The serpentinite multisystem revisited: chrysotile is metastable. Int. Geol. Rev. 46, 479–506.

Fletcher, R.C., Buss, H.L., Brantley, S.L., 2006. A spheroidal weathering model coupling porewater chemistry to soil thickness during steady-state denudation. Earth Planet. Sci. Lett. 244, 444–457.

Fletcher, R.C., Merino, E., 2001. Mineral growth in rocks: kinetic–rheological models of replacement, vein formation, and syntectonic crystallization. Geochim. Cosmochim. Acta 65, 3733–3748.

Frost, B.R., 1985. On the stability of sulfides, oxides, and native metals in serpentinite. J. Petrol. 26, 31–63.

Frost, B.R., Beard, J.S., 2007. On silica activity and serpentinization. J. Petrol. 48, 1351–1368.

Früh-Green, G.L., Kelley, D.S., Bernasconi, S.M., Karson, J.A., Ludwig, K.A., Butterfield, D.A., Boschi, C., Proskurowski, G., 2003. 30,000 years of hydrothermal activity at the Lost City vent field. Science 301, 495–498.

Gottschalk, M., 1997. Internally consistent thermodynamic data for rock-forming minerals in the system SiO_2–TiO_2–Al_2O_3–Fe_2O_3–CaO–MgO–FeO–K_2O–Na_2O–H_2O–CO_2. Eur. J. Mineral. 9, 175–223.

Hacker, B.R., 2008. H_2O subduction beyond arcs. G-Cubed, 9, http://dx.doi.org/10.1029/2007GC001707.

Hadley, K., 1976. Comparison of calculated and observed crack densities and seismic velocities in westerley granite. J. Geophys. Res. 81, 3483–3494.

Hänchen, M., Prigiobbe, V., Baciocchi, R., Mazzotti, M., 2008. Precipitation in the Mg-carbonate system: effects of temperature and CO_2 pressure. Chem. Eng. Sci. 63, 1012–1028.

Hatch, F.H., Wells, A.K., Wells, M.K., 1949. The Petrology of the Igneous Rocks. Thomas Murby and Co., London. (469 pp.).

Hilairet, N., Reynard, B., 2009. Stability and dynamics of serpentinite layer in subduction zone. Tectonophysics 465, 24–29.

Holland, T.B., Powell, R., 1990. An enlarged and updated internally consistent thermodynamic dataset with uncertainties and correlations: the system

K_2O–Na_2O–CaO–MgO–MnO–FeO–Fe_2O_3–Al_2O_3–TiO_2–SiO_2–C–H–O_2. J. Metamporphic Geol. 8, 89–124.
Iyer, K., Jamtveit, B., Mathiesen, J., Malthe-Sorenssen, A., Feder, J., 2008. Reaction-assisted hierarchical fracturing during serpentinization. Earth Planet. Sci. Lett. 267, 503–516.
Jamtveit, B., Austrheim, H., Malthe-Sorenssen, A., 2000. Accelerated hydration of the Earth's deep crust induced by stress perturbations. Nature 408, 75–78.
Jamtveit, B., Kobchenko, M., Austrheim, H., Malthe-Sorenssen, A., Royne, A., Svensen, H., 2011. Porosity evolution and crystallization-driven fragmentation during weathering of andesite. J. Geophys. Res. 116, B12204, http://dx.doi.org/10.1029/12011JB008649.
Jamtveit, B., Malthe-Sorenssen, A., Kostenko, O., 2008. Reaction enhanced permeability during retrogressive metamorphism. Earth Planet. Sci. Lett. 267, 620–627.
Johannes, W., 1969. An experimental investigation of the system MgO–SiO_2–H_2O–CO_2. Am. J. Sci. 267, 1083–1104.
Kelemen, P.B., Matter, J., Streit, E.E., Rudge, J.F., Curry, W.B., Bluztajn, J., 2011. Rates and mechanisms of mineral carbonation in peridotite: natural processes and recipes for enhanced, in situ CO_2 capture and storage. Annu. Rev. Earth Planet. Sci. 39, 545–576.
Kelemen, P.B., Matter, J.M., 2008. In situ carbonation of peridotite for CO_2 storage. Proc. Natl. Acad. Sci. USA 105, 17,295–217,300.
Lawn, B.R., Wilshaw, T.R., 1975. Fracture of Brittle Solids. Cambridge University Press, Cambridge UK (204 pp.).
Lindgren, W., 1912. The nature of replacement. Econ. Geol. 7, 521–535.
Ludwig, K.A., Shen, C.-C., Kelley, D.S., Cheng, H., Edwards, R.L., 2011. U–Th systematics and ^{230}Th ages of carbonate chimneys at the Lost City hydrothermal field. Geochim. Cosmochim. Acta 75, 1869–1888.
MacDonald, A.H., Fyfe, W.S., 1985. Rate of serpentinization in seafloor environments. Tectonophysics 116, 123–135.
Malthe-Sorenssen, A., Jamtveit, B., Meakin, P., 2006. Fracture patterns generated by diffusion controlled volume changing reactions. Phys. Rev. Lett. 96, 245501-1–245501-4.
Martin, B., Fyfe, W.S., 1970. Some experimental and theoretical observations on kinetics of hydration reactions with particular reference to serpentinization. Chem. Geol. 6, 185–202.
McCollom, T., 2007. Geochemical constraints on sources of metabolic energy for chemolithoautotrophy in ultramafic-hosted deep-sea hydrothermal systems. Astrobiology 7, 933–950.
McCollom, T.M., Sherwood Lollar, B., Lacrampe-Couloume, G., Seewald, J.S., 2010. The influence of carbon source on abiotic organic synthesis and carbon isotope fractionation under hydrothermal conditions. Geochim. Cosmochim. Acta 74, 2717–2740.
Misch, P., 1971. Porphyroblasts and "crystallization force": some textural criteria. Geol. Soc. Am. Bull. 82, 245–252.
Noiriel, C., Renard, F., Doan, M.-L., Gratier, J.-P., 2010. Intense fracturing and fracture sealing induced by mineral growth in porous rocks. Chem. Geol., 197–209.
O'Connor, W.K., Dahlin, D.C., Rush, G.E., Gerdemann, S.J., Nilsen, D.N., 2004. Final Report: Aqueous Mineral Carbonation, DOE/ARC-TR – 04 – 002. Office of Process Development, Albany Research Center, Office of Fossil Energy, US DOE, Albany, OR, 21 pp. plus appendices.
O'Hanley, D.S., 1992. Solution to the volume problem in serpentinization. Geology 20, 705–708.
Palandri, J.L., Kharaka, Y.K., 2004. A Compilation of Rate Parameters of Water–Mineral Interaction Kinetics for Application to Geochemical Modeling. US Geological Survey Open File Report 2004-1068, pp. 1–64.
Royne, A., Jamtveit, B., Mathiesen, J., Malthe-Sorenssen, A., 2009. Controls on rock weathering rates by reaction-induced hierarchical fracturing. Earth Planet. Sci. Lett. 275, 364–369.
Rudge, J.F., Kelemen, P.B., Spiegelman, M., 2010. A simple model of reaction induced cracking applied to serpentinization and carbonation of peridotite. Earth Planet. Sci. Lett. 291, 215–227.
Saldi, G.D., Jordan, G., Schott, J., Oelkers, E.H., 2009. Magnesite growth rates as a function of temperature and saturation state. Geochim. Cosmochim. Acta 73, 5646–5657.
Scherer, G.W., 2004. Stress from crystallization of salt. Cem. Concr. Res. 34, 1613–1624.
Seifritz, W., 1990. CO_2 disposal by means of silicates. Nature 345, 486.
Spiers, C.J., Schutjes, T.M., Brzesowsky, R.H., Peach, C.J., Liezenberg, J.L., Zwart, H.J., 1990. Experimental determination of constitutive parameters governing creep of rocksalt by pressure solution. Geol. Soc. London Spec. Publ. 54, 215–227.
Sprunt, E.S., Brace, W.F., 1974. Direct observation of microcavities in crystalline rocks. Int. J. Rock Mech. Min. Sci. Geomech. Abstr. 11, 139–150.
Steiger, M., 2005. Crystal growth in porous materials—I: the crystallization pressure of large crystals. J. Cryst. Growth 282, 455–469.
Stern, R.J., Smoot, N.C., 1998. A bathymetric overview of the Mariana forearc. The Island Arc 7, 525–540.
Taber, S., 1929. Frost heaving. J. Geol. 37, 428–461.
Tapponnier, P., Brace, W.F., 1976. Development of stress-induced microcracks in Westerly granite. Int. J. Rock Mech. Min. Sci. 13, 103–112.
Ulmer, P., Trommsdorff, V., 1995. Serpentine stability to mantle depths and subduction-related magmatism. Science 268, 858–861.
Walsh, J.B., 1965. The effect of cracks on the compressibility of rock. J. Geophys. Res. 70, 381–389.
Wong, T.F., 1982. Micromechanics of faulting in Westerly granite. Int. J. Rock Mech. Min. Sci. 19, 49–64.
Xu, W.Y., Apps, J.A., Pruess, K., 2004. Numerical simulation of CO_2 disposal by mineral trapping in deep aquifers. Appl. Geochem. 19, 917–936.
Yardley, B.W.D., 1974. Porphyroblasts and "crystallization force": discussion of some theoretical considerations. Geol. Soc. Am. Bull. 85, 61–62.
Zoback, M.D., Townend, J., 2001. Implications of hydrostatic pore pressures and high crustal strength for the deformation of intraplate lithosphere. Tectonophysics 226, 19–30.